

Structural and Conformational Properties of 1,2-Propadienylphosphine (Allenylphosphine) Studied by Microwave Spectroscopy and Quantum Chemical Calculations

Harald Møllendal,^{*,†} Jean Demaison,[‡] Denis Petitprez,[‡] Georges Wlodarczak,[‡] and Jean-Claude Guillemin[§]

Department of Chemistry, University of Oslo, P.O. Box 1033 Blindern, NO-0315 Oslo, Norway, Laboratoire de Physique des Lasers, Atomes et Molécules, UMR CNRS 8523, Bât. P5, Université de Lille1, F-59655 Villeneuve d'Ascq, France, and Laboratoire de Synthèse et Activation de Biomolécules, UMR CNRS 6052, Institut de Chimie de Rennes, ENSCR, F-35700 Rennes, France

Received: June 28, 2004; In Final Form: October 13, 2004

1,2-Propadienylphosphine (allenylphosphine), $\text{H}_2\text{C}=\text{C}=\text{CHPH}_2$, has been investigated by Stark and Fourier transform microwave spectroscopy. Two rotameric forms denoted syn and gauche have been assigned. The syn form has a symmetry plane (C_s symmetry) where the lone electron pair of phosphorus points toward the double bonds. The phosphino group is rotated roughly 120° from this position in the gauche rotamer. The dipole moment of syn was determined to be $\mu_a = 1.613(23)$, $\mu_b = 2.347(24)$, $\mu_c = 0$ (for symmetry reasons), and $\mu_{\text{tot}} = 2.848(28) \times 10^{-30}$ C m [0.854(8) D]. The energy difference between the two forms was found to be 2.1(4) kJ/mol from relative intensity measurements with syn as the more stable conformer. Extensive quantum chemical calculations have been carried out and accurate equilibrium structures have been determined for these two rotamers, as well as for the corresponding two conformers of vinylphosphine ($\text{H}_2\text{C}=\text{CHPH}_2$).

Introduction

The literature about the conformational and structural properties of aliphatic phosphines in the gas phase is not comprehensive presumably because these compounds are often toxic, pyrophoric, and unstable in air and they smell obnoxious. Microwave (MW) spectroscopic studies of $\text{CH}_3\text{CH}_2\text{PH}_2$,¹ $\text{H}_2\text{-PCH}_2\text{CH}_2\text{C}\equiv\text{N}$,² $\text{H}_2\text{PCH}_2\text{CH}_2\text{PH}_2$,³ $\text{HC}\equiv\text{CCH}_2\text{PH}_2$,⁴ $\text{H}_2\text{C}=\text{CHCH}_2\text{PH}_2$,⁵ $\text{H}_2\text{C}=\text{CHPH}_2$,⁶ and $\text{HC}\equiv\text{CPH}_2$ ⁷ have already demonstrated that aliphatic phosphines have unique conformational and structural properties different from those of the corresponding amines.

It is felt that the limited knowledge of this interesting class of compounds warrants further investigation. In this work, the studies of the aliphatic phosphines are extended to include 1,2-propadienylphosphine (allenylphosphine), $\text{H}_2\text{C}=\text{C}=\text{CHPH}_2$. The properties of this compound have previously been investigated by nuclear magnetic resonance, and infrared and high-resolution mass spectrometry,⁸ as well as by photoelectron spectroscopy supported by theoretical MNDO calculations.⁹ The photoelectron spectrum indicates that more than one conformer may be present in the gas phase.⁹

Rotation around the C–P bond leads to rotational isomerism in the title compound. Three typical conformations are drawn in Figure 1. A distinction between them may be made with reference to the lone electron pair (lep) of phosphorus. The C=C–P–lep has a syn-periplanar conformation in the syn conformer. It is anti-clinal in the gauche form, and anti-periplanar in the anti form. The syn and anti forms will thus each have a symmetry plane (C_s symmetry), whereas the gauche form has no symmetry (C_1 point group).

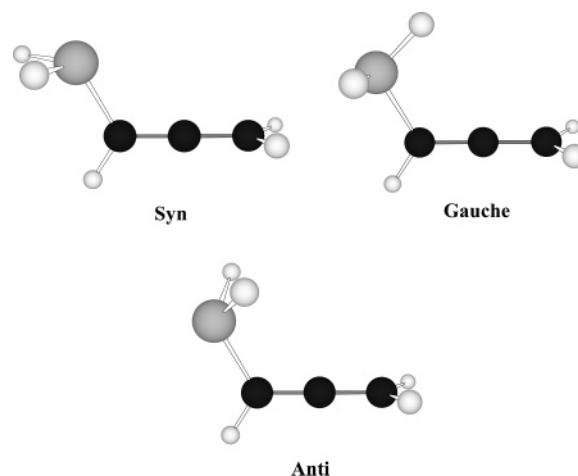


Figure 1. Possible rotameric forms of allenylphosphine. The syn and gauche conformers were assigned in this work. Anti represents a transition state.

It should be mentioned that an extensive delocalization of the lone pair of phosphorus into the π -electron system of the allenyl moiety might lead to yet a fourth planar (or nearly planar) conformation for the $-\text{C}=\text{CHPH}_2$ group of atoms. This hypothetical conformation is not drawn in Figure 1.

In the vinylphosphine molecule ($\text{H}_2\text{C}=\text{CHPH}_2$), two conformers were identified in MW investigations.^{6,7} Interestingly, the most stable one of these is similar to the syn form of Figure 1, whereas the less stable form is similar to gauche. No experimental determination was made of the energy difference, but the former conformer is the more stable one. Ab initio calculations yielded an energy difference in the 1.7–5.4 kJ/mol range between these two forms depending on the level of calculation.⁷

The electronic environment in the allenyl group is of course rather different from that of the vinyl group because two double

* Corresponding author. E-mail: harald.mollendal@kjemi.uio.no. Tel: +47 22 85 56 74. Fax: +47 22 85 54 41.

[†] University of Oslo.
[‡] Université de Lille1.
[§] ENSCR.

bonds adjacent to one another are present in the former compounds, while only one such bond is found in the latter molecules. This difference between allenic and vinylic phosphines might influence the conformational as well as other molecular properties. Moreover, no allenic phosphine has previously been studied by the very specific MW spectroscopic method. These were the main reasons for choosing the prototype of allenic phosphines, allenylphosphine, for study.

The methods of investigation were in addition to MW spectroscopy, quantum chemical calculations. The extremely high resolution and specificity of the former method are ideal for analyzing conformational mixtures. Modern quantum chemical calculations are now rather reliable and may provide information not readily available from experiments alone, thus supplementing MW spectroscopy in an ideal manner. Comprehensive quantum chemical calculations have in the present case been carried out to predict a number of molecular properties including an accurate equilibrium structure not only for the title compound, but for vinylphosphine as well.

Experimental Section

Synthesis of 1,2-Propadienylphosphine (Allenylphosphine).

Caution: The 1,2-propadienylphosphine is pyrophoric and potentially highly toxic. All reactions and handling should be carried out in a well-ventilated hood.

The synthesis of allenylphosphine has already been reported.⁸ The apparatus was similar to the one described for the preparation of 2-propynylphosphine.⁴ The reducing agent (AlHCl₂) was prepared as follows: in a 250-mL two-necked flask equipped with a nitrogen inlet and a stirring bar were introduced LiAlH₄ (1.14 g, 30 mmol) and tetraglyme (50 mL). The flask was immersed in a cold bath (−30 °C) and aluminum chloride (12.0 g, 90 mmol) was added by portions.¹⁰ The flask was fitted on the vacuum line, allowed to warm to −10 °C, and degassed. The 5,5-dimethyl-2-oxo-2-(propa-1',2'-diene)-1,3,2-dioxaphosphorinane⁸ (1.88 g, 10 mmol) dissolved in tetraglyme (50 mL) was slowly added with a flex-needle through the septum in about 20 min. During and after addition, the formed allenylphosphine was distilled off in vacuo from the reaction mixture. A cold trap (−80 °C) selectively removed less volatile products and the phosphine was condensed in a second cold trap (−120 °C) to remove the most volatile products (mainly PH₃). After the sample was disconnected from the vacuum line by stopcocks, the product was kept at low temperature (< −30 °C) before analysis. The allenylphosphine was thus obtained in 92% purity and in a 77% yield (0.55 g). The presence of several other phosphines in a 0.1–5% yield cannot be avoided. The main impurity was the 2-propenylphosphine (≈4%).

Stark Spectrometer Experiment. The MW spectrum was studied using the Oslo Stark spectrometer, which is described briefly in ref 11. A 3-m Stark cell made of brass was utilized. Radio frequency microwave double resonance (RFMWDR) experiments were carried out as described in ref 12 using the equipment mentioned in ref 13. The 8–62 GHz spectral region was investigated with the cell cooled to dry ice temperature (−78 °C). The pressure was a few pascals when the spectrum was recorded and stored electronically using the program written by Waal.¹⁴ The accuracy of the spectral measurements was better than ±0.10 MHz and the maximum resolution was about 0.4 MHz.

The compound was kept for several months in a refrigerator at about −30 °C when not in use. Polymeric products were seen to form slowly. However, the compound showed no signs of

TABLE 1: Spectroscopic Constants and Dipole Moment of Allenylphosphine as Calculated at the B3LYP/6-311G(3df,2pd) Level of Theory

	syn	gauche
<i>A</i> /MHz	25705.8	26021.4
<i>B</i> /MHz	2740.4	2714.1
<i>C</i> /MHz	2573.3	2544.8
$\mu_a/10^{-30}$ C m	2.06	2.37
$\mu_b/10^{-30}$ C m	2.25	0.10
$\mu_c/10^{-30}$ C m	0.0	1.51
$\mu_{tot}/10^{-30}$ C m	3.29	2.82
Δ_J /kHz	1.180	1.066
Δ_{JK} /kHz	−44.60	−44.16
Δ_K /kHz	818.3	830.4
δ_J /kHz	0.198	0.180
δ_K /kHz	−2.347	3.856

decomposition in the brass in the course of 6–8 h. The MW spectra of impurities of 2-propenylphosphine, H₂=CH–CH₂–PH₂,⁵ as well as impurities of unidentified origin were noted.

Microwave Fourier Transform Spectrometer Experiments. Rotational spectra in the 5–20 GHz spectral range were recorded with the Lille microwave Fourier transform (MWFT) spectrometer.¹⁵ A gas mixture of 100 Pa of allenylphosphine completed with neon as carrier gas to a total pressure of 1 × 10⁵ Pa was prepared. Gas pulses were then expanded into the vacuum tank through a pulsed nozzle to create a supersonic jet parallel to the optical axis of the Fabry–Perot cavity. The pulsed valve was opened for 600 μs at a repetition rate of 1.5 Hz. To polarize the allenylphosphine molecule, 2 μs microwave pulse were used with power fields of 0.8 mW for the syn form transitions and 0.5 mW (1 mW) for the μ_a type (μ_c type, respectively) gauche rotamer transitions. A total of 4096 data points per free emission decay are collected at a 10 MHz sample rate, which gives, after Fourier transformation, a spectral resolution of 2.4 kHz per point. The accuracy of frequency measurements is estimated to be better than 3 kHz.

Results and Discussion

Computational Methods. The majority of the quantum chemical calculations were made in Lille with the MolPro2000¹⁶ and Gaussian03 programs.¹⁷ A few calculations were also performed in Oslo using the latter program.

To obtain a first prediction of the rotational constants, density functional theory with the hybrid functional B3LYP (Becke's three parameter¹⁸ functional employing the Lee, Yang and Parr correlation functional¹⁹) was used with the 6-311G(d,p) basis set as implemented in Gaussian 03. To improve the accuracy of the predicted rotational spectra, the structure, the harmonic force field, and the quartic centrifugal distortion constants were next calculated at the B3LYP/6-311G(3df,2pd) level of theory. The results are given in Table 1.

The Gaussian-3 (G3) theory²⁰ was employed to calculate the energy differences between the conformers (Figure 1). The zero-point energy (ZPE) is first calculated at the Hartree–Fock level of theory (HF/6-31G(d)) followed by a scaling of the vibrational frequencies (scaling factor: 0.8929). G3 theory uses, as reference geometry, the geometry from MP2/6-31G(d) level of theory, and all electrons are correlated. The quadratic configuration interaction, QCISD(T), energy²¹ at a large basis set is obtained assuming that a series of calculations at lower level of theories are additive.²² The total energy at 0 K may be expressed as

$$E_0(\text{G3}) = \text{MP4}/d + [\text{QCISD}(\text{T})/d - \text{MP4}/d] + \\ [\text{MP4}/\text{plus} - \text{MP4}/d] + [\text{MP4}/2df,p - \text{MP4}/d] + \\ [\text{MP2}(\text{FU})/\text{G3L} - \text{MP2}/2df,p - \text{MP2}/\text{plus} + \text{MP2}/d] + \\ E(\text{ZPE}) + E(\text{HLC})$$

where MP4 = fourth-order Møller Plesset,²³ $d = 6\text{-}31\text{G}(\text{d})$, plus = $6\text{-}31\text{+G}(\text{d})$, $2df,p = 6\text{-}31\text{G}(2df,p)$, G3L = G3Large basis set, and $E(\text{HLC})$ is a higher level correction depending on the numbers of α - and β -electrons. Thus, it cancels out when we make the difference between the energies of two conformers. Finally, FU = full, meaning that all electrons are correlated.

The G3 calculations were repeated for the structurally similar compound vinylphosphine, $\text{H}_2\text{PCH}=\text{CH}_2$, which was studied previously.^{6,7} The results are given in Table 2. This table also includes the results found in the MP2/6-311G(3df,p) calculations.²⁴

It is noted that the most stable form is obtained when the phosphorus lcp is syn-periplanar (syn) with respect to the C–C–P link of atoms for both allenyl- and vinylphosphine. The lep-anti-clinal form (gauche) is less stable and the lep-anti-periplanar form (anti) is a transition state in both compounds. The barrier between the two gauche forms is low. The anticlinal form represents a maximum on the potential energy hyper surface in both molecules. This conformation has an energy that is 7.5 kJ/mol higher than the energy of syn in allenylphosphine and 11–12 kJ/mol higher in vinylphosphine (Table 2). Another transition state occurs about 65° from syn with an energy 6–7 kJ/mol higher than the energy of syn. For vinylphosphine, the results are in extremely good agreement with the previous results that were obtained at the MP2/6-311G(3df,p) level of theory.²⁴

Structures. For the calculation of the geometrical structures, the second-order Møller–Plesset perturbation theory, MP2,²³ and the coupled-cluster method with single and double excitation²⁵ augmented by a perturbational estimate of the effects of the connected triple excitations,²⁶ CCSD(T), was used with the Dunning's correlation consistent polarized valence basis sets, cc-pV($n+d$)Z with $n = \text{D, T, Q}$.²⁷

The structure of both stable forms of allenylphosphine and vinylphosphine was first calculated at the MP2/cc-pV(Q+d)Z level of theory. This method is known to give reliable angles.²⁸ On the other hand, the bond lengths are affected by a small error, which is mainly systematic. This error (also called offset) may be most easily estimated with the help of small molecules whose structure is accurately known and can be used to correct ab initio bond lengths. To determine the offsets of the $r(\text{C}=\text{C})$ and $r(\text{C}-\text{H})$ bond lengths, we have used allene, $\text{H}_2\text{C}=\text{C}=\text{CH}_2$, whose structure is well-known.²⁹ Likewise, for the $r(\text{P}-\text{H})$ bond length, we have used phosphine, PH_3 .³⁰

For the $r(\text{C}-\text{P})$ bond length, we have calculated the ab initio equilibrium structure of vinylphosphine. As this molecule is smaller than allenylphosphine, it is more easily amenable to high level ab initio calculations. For this reason, the structure of the syn form of vinylphosphine was first calculated at the CCSD(T) level of theory, but the expensive calculation at the CCSD(T)/cc-pV(Q+d)Z level was replaced by simpler calculations because it is well established that the variation from CCSD(T)/cc-pV(T+d)Z to CCSD(T)/cc-pV(Q+d)Z may be accurately predicted with MP2 calculations.^{29,31} The following approximation formula was used:

$$r[\text{CCSD}(\text{T})/\text{cc-pVQZ}] = r[\text{CCSD}(\text{T})/\text{cc-pVTZ}] + \\ r[\text{MP2}/\text{cc-pVQZ}] - r[\text{MP2}/\text{cc-pVTZ}]$$

The coupled cluster T_1 diagnostic,³² which is 0.012 at the CCSD-

TABLE 2: Relative Energies (kJ/mol) of the Different Conformers of Allenylphosphine and Vinylphosphine

	allenylphosphine ^a		vinylphosphine ^a		vinylphosphine ^b	
	ΔE	τ^c	ΔE	τ^c	ΔE	τ^c
syn	0.0	0.0	0.0	0.0	0.0	0.0
TS ^d	6.23	65.3	6.26	62.8	6.92	63.9
gauche	2.47	119.5	2.12	113.1	2.15	111.2
anti ^d	7.46	180.0	11.17	180.0	11.94 ^e	180.0

^a G3 calculations; see text. ^b MP2/6-311G(3df,p) calculations.²⁴ ^c τ is the dihedral angle (in degrees) between the lone pair and the C=C(H)P skeleton. ^d TS and anti are transition states (imaginary torsional frequency). ^e A MP4/6-311G(3df,p) calculation gives 11.44 kJ/mol.²⁴

TABLE 3: Equilibrium Structures^a of the Syn and Gauche Forms of Vinylphosphine^b

	syn ^c	gauche ^{d,e}
$r(\text{C}_1=\text{C}_2)$	133.5	133.5
$r(\text{C}_1-\text{P})$	182.4	181.9
$r(\text{C}_2-\text{H}_{\text{cis}})$	108.2	108.2
$r(\text{C}_2-\text{H}_{\text{trans}})$	108.2	108.1
$r(\text{C}_1-\text{H})$	108.3	108.5
$r(\text{P}-\text{H})$	141.4	
$r(\text{P}-\text{H}_{\text{oop}})$		141.3
$r(\text{P}-\text{H}_{\text{ip}})$		141.3
$\angle(\text{C}_1\text{C}_2\text{H}_{\text{cis}})$	121.1	121.6
$\angle(\text{C}_1\text{C}_2\text{H}_{\text{trans}})$	121.6	121.2
$\angle(\text{HC}_1\text{C}_2)$	119.6	119.0
$\angle(\text{C}_2\text{C}_1\text{P})$	120.3	125.4
$\angle(\text{HPC}_1)$	97.4	
$\angle(\text{H}_{\text{oop}}\text{PC}_1)$		97.7
$\angle(\text{H}_{\text{ip}}\text{PC}_1)$		97.0
$\angle(\text{HC}_1\text{PH})$	46.8	
$\angle(\text{PC}_1\text{C}_2\text{H}_{\text{cis}})$		5.6
$\angle(\text{PC}_1\text{C}_2\text{H}_{\text{trans}})$		-174.3
$\angle(\text{HC}_1\text{C}_2\text{H}_{\text{trans}})$		-0.6
$\angle(\text{C}_2\text{C}_1\text{PH}_{\text{ip}})$		-19.2
$\angle(\text{C}_2\text{C}_1\text{PH}_{\text{oop}})$		71.5

^a See text. ^b Distances in pm and angles in degrees. ^c CCSD(T)/V(T+d)Z + MP2[V(Q+d)Z - V(T+d)Z] + MP2(ae)/CVQZ - MP2(fc)/CVQZ; see Table 7S in Supporting Information for details of calculations. ^d Core correlation taken from the syn conformer; see Table 3. ^e CCSD(T)/V(T+d)Z + MP2[V(Q+d)Z - V(T+d)Z] + core correlation; see also Table 8S in Supporting Information for details of calculations.

(T)/cc-pV(T+d)Z level, indicates that nondynamical electron correlation is not important and that the CCSD(T) results should be reliable.

To estimate the core and core-valence correlation effects on the computed molecular geometry, the correlation-consistent polarized core-valence quadruple- ζ basis set, cc-pCVQZ,³³ was employed with the MP2 method which is known to be a rather satisfactory approximation,³¹ at least for bonds involving only first-row atoms. This correction leads to the expected bond shortenings. The derived equilibrium structure for the syn and gauche forms of vinylphosphine is given in Table 3. Further data are found in Supporting Information, Tables 7S and 8S. The equilibrium structure of the gauche form was calculated from the ab initio CCSD(T) structure assuming that the core correlation is the same as for the syn conformer, which is likely to be a safe approximation.

Finally, the structures of the syn and gauche forms of allenylphosphine are given in Table 5. They are calculated from the ab initio MP2/cc-pV(Q+d)Z structures with the offset corrections given in Table 4 and calculated as discussed above. See also Supporting Information, Tables 9S and 10S.

A careful examination of the offsets shows that they are not exactly constant for a given bond. For instance, for the P–H

TABLE 4: Determination of the Offsets for the MP2/cc-pV(Q+d)Z Ab Initio Structures (Distances in pm and Angles in Degree)

molecule	bond	ab initio ^a	r_e	offset ^b	ref ^c
H ₂ C=CHPH ₂	C–P	182.09	182.44	0.35	this work
PH ₃	P–H	140.93	141.14	0.21 ^d	29
H ₂ C=C=CH ₂	C=C	130.59	130.67	0.08 ^e	28
H ₂ C=C=CH ₂	C–H	108.00	108.11	0.11	28

^a MP2(fc)/cc-pV(Q+d)Z. ^b $r_e - r$ (ab initio). ^c For the equilibrium structure. ^d 0.29 pm from H₂C=CHPH₂; see Table 3. ^e 0.04 pm from H₂C=CHPH₂; see Table 8S in Supporting Information for details of calculations.

TABLE 5: Equilibrium Structures^a of the Syn and Gauche Forms of Allenylphosphine^b

	syn ^c	gauche ^c
$r(\text{C}_1\text{--P})$	182.9	182.9
$r(\text{C}_1\text{=C}_2)$	130.9	130.7
$r(\text{C}_2\text{=C}_3)$	130.7	130.9
$r(\text{C}_1\text{--H})$	108.4	108.5
$r(\text{P--H})$	141.3	
$r(\text{P--H}_{\text{oop}})$		141.3
$r(\text{P--H}_{\text{ip}})$		141.0
$r(\text{C}_3\text{--H})$	108.1	
$r(\text{C}_3\text{--H}_{(-)})$		108.2
$r(\text{C}_3\text{--H}_{(+)})$		108.2
$\angle(\text{PC}_1\text{C}_2)$	119.3	123.5
$\angle(\text{C}_1\text{C}_2\text{C}_3)^c$	178.6	178.6
$\angle(\text{C}_2\text{C}_1\text{H})$	119.3	119.2
$\angle(\text{C}_1\text{PH})$	97.2	
$\angle(\text{C}_1\text{PH}_{\text{oop}})$		97.9
$\angle(\text{C}_1\text{PH}_{\text{ip}})$		96.5
$\angle(\text{HPH})$	92.7	94.3
$\angle(\text{C}_2\text{C}_3\text{H})$	120.7	
$\angle(\text{C}_2\text{C}_3\text{H}_{(-)})$		120.9
$\angle(\text{C}_2\text{C}_3\text{H}_{(+)})$		120.7
$\angle(\text{HC}_3\text{H})$	118.6	118.4
$\angle(\text{C}_2\text{C}_1\text{PH})$	133.2	
$\angle(\text{C}_2\text{C}_1\text{PH}_{\text{oop}})$		108.0
$\angle(\text{C}_2\text{C}_1\text{PH}_{\text{ip}})$		12.8
$\angle(\text{PC}_1\text{C}_3\text{H})$	89.7	
$\angle(\text{PC}_1\text{C}_3\text{H}_{(-)})$		84.2
$\angle(\text{HC}_1\text{C}_3\text{H}_{(-)})$		-89.2
$\angle(\text{PC}_1\text{C}_3\text{H}_{(+)})$		-95.4

^a See text. ^b Distances in pm and angles in degrees. ^c MP2/cc-pV(Q+d)Z with offsets of Table 4; see also Tables 9S and 10S in Supporting Information. ^d P inside the acute angle.

bond length, the offset is 0.21 pm in PH₃ and 0.35 pm in vinylphosphine (syn form, Table 4). The offset is indeed only approximately constant for a given bond and is known to be sensitive to the chemical environment.

Furthermore, the core correlation was calculated at the MP2 level for vinylphosphine. This approximation is known to give a core correlation slightly too large for bond lengths where a second-row atom (here P) is involved.³⁴

Accuracy of the Estimated Equilibrium Structures. The accuracy of the estimated equilibrium structures in Tables 3 and 5 warrants comments. The bond lengths and angles not involving the phosphorus atom are estimated to be accurate to within 0.3 pm and 0.2°, respectively. Bond lengths and angles involving the phosphorus atom are likely to be slightly less accurate, as the following will show.

The ground-state rotational constants determined for the two forms in the experimental section below are obviously insufficient to determine the full structure of allenylphosphine. These experimental constants determined for the ground vibrational state usually deviate by less than about 1% from the equilibrium rotational constants. Moreover, the rotational constants calcu-

TABLE 6: Experimental Ground State and Calculated Equilibrium Rotational Constants (MHz)

	Gs ^a	Eq ^b	Gs–Eq ^c	Gs–Eq ^d
Vinylphosphine Syn				
A	39899.31	40246.92	-347.6	-595.25
B	5521.90	5542.60	-20.7	-13.51
C	5055.04	5077.83	-22.8	-33.42
Vinylphosphine Gauche				
A	40484.15	40699.8	-215.6	-215.31
B	5458.08	5489.31	-31.2	-42.36
C	4974.19	5004.62	-30.4	-39.25
Allenylphosphine Syn				
A	25004.08	24836.1	168.0	-175.18
B	2765.72	2781.34	-15.6	-5.37
C	2586.27	2600.23	-14.0	-8.46
Allenylphosphine Gauche				
A	25334	25051.1	282.9	-18.27
B	2735.98	2755.3	-19.3	-14.01
C	2555.22	2571.39	-16.2	-14.00

^a Experimental ground-state constants taken from refs 6 and 7 in the case of vinylphosphine, or from Tables 7 and 9 in the case of the title compound. ^b Equilibrium constants from the estimated equilibrium structures; see Tables 3 and 5. ^c $B_0^g(\text{exp}) - B_e^g(\text{calc})$. ^d $B_0^g - B_e^g$ calculated at the MP2/6-31G* level of theory. For the syn form of vinylphosphine, the corrections at the MP2/6-311G(3df,2p) are $A_0 - A_e = -565$, $B_0 - B_e = -12.6$, and $C_e - C_0 = -32.3$ MHz, respectively.

lated from the equilibrium structure are generally larger than the ground-state rotational constants.

The two kinds of rotational constants are compared in Table 6. It is seen that they agree well within the 1% limit. However, it is seen that the experimental values for the A rotational constants of the two conformers of allenylphosphine is larger than the A rotational constants calculated from the equilibrium structure. This is contrary to the usual situation, as already noted.

To check this unusual behavior, we have calculated the difference between the experimental and calculated rotational constants ($B_0^g(\text{exp})$, $g = a, b, c$) at the MP2/6-31G* level. The results are given in the last column of Table 5. It is seen that the expected negative difference is indeed calculated for the A rotational constants, and there is reasonably good agreement for the other rotational constants.

The A rotational constants of syn and gauche allenylphosphine are very sensitive to the coordinates of the phosphorus atom. A slight modification of the C–P bond length and C–C–P bond angle of the equilibrium structures given in Table 5 would produce better agreement. The uncertainty of these two parameters are thus estimated to be 0.5 pm and 0.4°, compared to 0.3 pm and 0.2°, respectively, for the remaining bond lengths and angles.

Stark Spectrum and Assignment of the Syn Rotamer. The first survey spectra taken using Stark spectroscopy revealed a rather rich and comparatively intense MW spectrum. The syn conformer (Figure 1) was predicted by the quantum chemical calculations above to be the preferred form of the molecule. μ_b was calculated to be the largest component of the dipole moment for this form (Table 1). Using the B3LYP/6-311G(3df,2pd) rotational constants available in the initial phase of this work, the strong ^bQ-branch series $J_{0,J} \leftarrow J_{1,J-1}$ was predicted to have a number of transitions at frequencies higher than 23 GHz. These transitions were soon identified. Their assignments were confirmed by their fit to Watson's Hamiltonian (A reduction, I' representation)³⁵ and the fact that the Stark effects of several of them were well-resolved.

Searches for low-J a- and b-type R-branch lines were made next and soon met with success. The assignments of some of

TABLE 7: Rotational (MHz), Quartic Centrifugal Distortion (kHz), and Sextic Centrifugal Distortion Constants (Hz)^a of the Syn Conformer of Allenylphosphine

vib state	ground	C–P torsion	lowest bending vib
<i>A</i>	25004.0803(23)	24801.0003(87)	25363.120(11)
<i>B</i>	2765.72333(23)	2765.76500(97)	2774.8108(12)
<i>C</i>	2586.26670(27)	2586.6823(10)	2590.3128(13)
Δ_J	1.30883(65)	1.3114(12)	1.3031(15)
Δ_{JK}	−48.964(15)	−49.018(26)	−49.358(31)
Δ_K	818.33(13)	740.85(15)	922.72(21)
δ_J	0.23074(13)	0.23279(23)	0.23351(23)
δ_K	1.570(39)	−1.900(51)	4.433(27)
Φ_J	0.00276(18)	−0.00220(36)	0.00075(51)
Φ_{JK}	−0.1396(54)	−0.363(11)	−0.152(18)
ϕ^b	0.001036(50)	0.000500(79)	0.001121(82)
$(I_a + I_b - I_c)^c$	7.532580(10)	7.726725(28)	6.953250(33)
N^d	344	229	176
rms^e	0.016 ^f	0.099 ^g	0.108 ^g

^a A reduction I' representation.³⁵ B3LYP/6-311G(3df,2pd) predictions of rotational constants and quartic centrifugal distortion constants are found in Table 1. Rotational constants calculated from the equilibrium structure are listed in Table 6. ^b Further sextic constants preset at zero. ^c Moments of inertia with dimension 10^{-20} m² u. Conversion factor: 5053.7905 nm² u MHz. ^d Number of lines used in the fit. ^e Root-mean-square deviation. ^f From weighted fit; see text. ^g From fit with equal weights.

them were confirmed both by Stark effect studies and fit to the said Hamiltonian. The assignments of some of the *a*-*R*-transitions were also confirmed by RFMWDR experiments.

The assignments were then gradually extended to include increasingly higher-*J* transitions. Ultimately, about 350 lines of the *a*- and *b*-varieties with a maximum value of *J* = 78 were assigned. Even higher-*J* transitions were searched for, but their intensities were presumably too low to allow unique identifications to be made. *c*-type lines were also searched for, but not found presumably because the corresponding dipole moment component is identical to zero owing to the *C_s* symmetry of the syn conformer.

Another 14 lines were found next using Fourier transform spectroscopy. Ultimately 344 *a*- and *b*-type transitions were used to determine the spectroscopic constants shown in Table 7. Three sextic centrifugal distortion constants had to be used in addition to the five quartic centrifugal distortion constants to get a fit consistent with the measurements accuracy. The accuracy of the transitions measured using the Fourier transform and Stark spectroscopy are different, and weights have therefore been applied in the fitting procedure. The inverse square of the uncertainties have been used. The full spectrum including the uncertainties is shown in Supporting Information, Table 1S. The maximum centrifugal distortion is rather prominent amounting to more than 5 GHz for the highest-*J* transitions.

Comparison of the B3LYP/6-311G(3df,2pd) rotational constants (Table 1) predicted for syn and their experimental counterparts (Table 7) shows expected agreement (2.8% for *A*, 0.8% for *B*, and 0.5% for *C*, respectively) for calculations of this level of theory. The agreement between the theoretical and experimental quartic centrifugal distortion constants given in the same tables is about 1 order of magnitude poorer, as expected.

Vibrationally Excited States of Syn. The vibrationally excited states of this rotamer was assigned using the Stark-modulated spectrometer. The ground-state transitions of syn were accompanied by two series of lines showing Stark and RFMWDR patterns similar to the corresponding transitions belonging to the ground vibrational state but having considerably less intensity. These transitions were assumed to belong to

TABLE 8: Second-Order Stark Coefficients^a and Dipole Moment of the Syn Conformer of Allenylphosphine

transition	M	stark coefficients $\Delta E^{-2}/10^{-5}$ MHz V^{-2} cm ²	
		obsd	calcd
1 _{1,0} ← 1 _{0,1}	1	8.73(10)	8.90
2 _{1,1} ← 2 _{0,2}	2	1.76(3)	1.60
3 _{1,2} ← 3 _{0,3}	3	0.720(8)	0.736
	2	0.427(6)	0.440
4 _{1,3} ← 4 _{0,4}	4	0.542(6)	0.532
5 _{1,4} ← 5 _{0,5}	5	0.453(5)	0.459
	4	0.218(3)	0.208
6 _{1,5} ← 6 _{0,6}	6	0.441(2)	0.421
	5	0.253(3)	0.256
dipole moment			
$\mu_a = 1.613(23)$, $\mu_b = 2.347(24)$, $\mu_c = 0^b$ and $\mu_{\text{tot}} = 2.848(28) \times 10^{-30}$ C m			

^a Uncertainties represent one standard deviation. 1 D = 3.33564 10^{-30} C m. B3LYP/6-311G(3df,2pd) values are listed in Table 1. ^b Preset at this value in the least-squares fit.

vibrationally excited states. The assignments were made in the same manner as described for the ground vibrational state. Only *a*- and *b*-type lines were found as expected. The spectroscopic constants are shown in Table 7. The transitions of the excited states were assigned unit weights in the fitting procedure. The full spectra are listed in Supporting Information, Tables 2S and 3S.

It is seen in Table 7 that one of the excited states is assigned as the first excited state of the lowest torsional mode, viz the torsion around the P–C bond. This assignment has been made because $I_a + I_b - I_c$ increases upon excitation to 7.62 from the ground-state value of 7.53×10^{-20} u² (Table 8). An increase is expected for a torsional vibration.³⁶ Relative intensity measurements were made observing the precautions of ref 37. A frequency of 137(25) cm^{−1} was obtained for this normal mode. This should be compared to 122 cm^{−1} obtained in the theoretical B3LYP calculations above but not tabulated.

The other vibrationally excited state is assigned as the first excited state of the lowest bending vibration. This assignment has been made because $I_a + I_b - I_c$ now decreases to 6.95×10^{-30} u² as expected for this kind of vibration.³⁷ Relative intensity measurements yielded 156(25) cm^{−1} for this mode, relatively close to the theoretical value (169 cm^{−1}).

Dipole Moment. The dipole moment of syn was determined in a least-squares fit using the second-order Stark coefficient of the transitions shown in Table 8. The weight of each Stark coefficient was taken to be the inverse square of the standard deviation of that coefficient, which is also shown in the same table. Only μ_a and μ_b were allowed to vary in the fit, while μ_c was kept constant at zero because of the symmetry plane. The cell was calibrated using OCS, whose dipole moment was taken to be $2.3857(68) \times 10^{-30}$ C m.³⁸

The experimental values of the dipole moment along the principal inertial axes $\mu_a = 1.613(23)$, $\mu_b = 2.347(24)$ and $\mu_{\text{tot}} = 2.848(28) \times 10^{-30}$ C m agree reasonably well with the both the B3LYP predictions (Table 1) and with advanced MP2/cc-pV(Q+d)Z calculations, which yielded $\mu_a = 1.744$, $\mu_b = 2.813$, and $\mu_{\text{tot}} = 3.310 \times 10^{-30}$ C m. These theoretical values are additional evidence that syn has indeed been assigned and not confused with gauche or anti, which would have had significantly different principal-axis dipole moment components.

Fourier Transform Spectrum and Assignment of the Gauche Rotamer. There are two identical gauche forms separated by a mirror plane. Tunneling of the phosphino group

TABLE 9: Rotational (MHz) and Quartic Centrifugal Distortion (kHz)^a of the Ground Vibrational State of the Gauche Conformer of Allenylphosphine

<i>A</i>	25334(19)
<i>B</i>	2735.9789(49)
<i>C</i>	2555.2237(50)
Δ_J	1.163(12)
Δ_{JK}	-46.874(32)
Δ_K	830.4 ^b
δ_J	0.180 ^b
δ_K	3.856 ^b
$(I_a + I_b - I_c)^c$	6.882(15)
N^d	74
rms ^e /MHz	0.097

^a Comments as for Table 7. ^b Preset at this value taken from Table 1. ^c Moments of inertia with dimension 10^{-20} m² u. Conversion factor: 5053.7905 nm² u MHz. ^d Number of lines used in the fit. ^e Root-mean-square deviation.

will transform one form into its mirror image. A double-minimum potential is associated with this transformation. Each vibrational state is thus split into two components. The lowest energy component of the ground vibrational state is denoted the (+)-state, whereas the higher energy component is denoted the (-)-state. *a*-type transitions will obey ordinary rotational transitional rules plus (+) \leftarrow (+), resulting in two closely spaced transitions separated by a few megahertz at most. The *c*-type lines obey ordinary rotational selection rules plus (-) \leftarrow (+), or (+) \leftarrow (-). This leads to comparatively much larger splittings for *c*-type lines than in the case of the *a*-type transitions.

The $J = 1 \leftarrow 0$, $J = 2 \leftarrow 1$ and $J = 3 \leftarrow 2$ *a*-type series of transitions of the gauche rotamer was readily assigned using the Fourier transform spectrometer. Splittings were resolved for most, but not all, of these transitions, as can be seen in Table 4S in Supporting Information. The largest splitting is 1.646 MHz found for the $2_{1,2} \leftarrow 1_{1,1}$ transition (Table 4S). The splittings of those transitions that were not resolved are less than 10 kHz.

Attempts to fit these ^a*R*-lines to Watson's Hamiltonian³⁵ within the measurement accuracy of 3 kHz failed. The reason for this is presumed to be coupling between rotation and tunneling, which is often seen in such cases. This coupling makes it impossible to assign correctly the (+) or the (-) label to each of the split lines in Table 4S (Supporting Information).

The first tentative spectroscopic constants obtained from *a*-type lines in Table 4S were next used to predict further ^a*R*-transitions involving higher-*J* transitions. These transitions appear at frequencies not accessible for the Fourier transform spectrometer. Their assignments were now readily achieved using the Stark-modulated spectrometer. Transitions involving *J* up to $J = 11$ were found in this way. None of these appeared to be significantly perturbed by tunneling. The assignments of these transitions were confirmed not only by their fit to the Watson Hamiltonian,³⁵ but by RFMWDR experiments, Stark modulation patterns, partially resolved Stark effects and intensities as well. The spectrum used to determine the spectroscopic constants of the gauche rotamer is found in Table 5S in Supporting Information. Some of the low-*J* lines measured by Fourier transform spectroscopy have been included in the fit. Their average frequencies have been used in these cases. Unit weights were applied in the fitting of these transitions because the amount of tunneling perturbation is unknown. The spectroscopic constants derived from the ^a*R*-lines are listed in Table 9. Only two quartic centrifugal distortion constants Δ_J and Δ_{JK} were fitted. The remaining quartic constants were fixed at the theoretical values shown in Table 1. The agreement between the calculated (Table 1) and experimental values for Δ_J and Δ_{JK} (Table 9) is satisfactory.

The gauche rotamer is predicted to have a sizable dipole moment component along the *c*-axis according to the calculations (Table 1). The strongest *c*-type lines are in general several series of different Q-branch transitions. The *c*-type transitions were believed to be split into two components owing to tunneling of the phosphino group, just as observed for the related molecule vinylphosphine,⁶ where a splitting of about 9 MHz was observed. Extensive searches were now carried out in an attempt to find these split transitions. These attempts met with partial success. Several lines of the $J_{1,J} \leftarrow J_{0,J}$ *c*-type series with *J* between 4 and 22 are assumed to have been assigned. They are listed in Table 6S (Supporting Information). All these transitions are either of the (+) \leftarrow (-) species, or of the (-) \leftarrow (+) species, but it is not possible to know which one of these two alternatives is correct. Attempts to find the other species, which would have allowed a unique identification, failed, possibly because the splittings are large or perturbed. Searches were also made for further *c*-type Q- and R-branch lines of this rotamer, however, with a negative result. The dense and complicated nature of this perturbed spectrum in addition to the relative weakness of these *c*-type lines rendered this search unsuccessful. Searches were also made for *b*-type lines, but none were found presumably because μ_b is close to zero (Table 1).

Energy Difference. The energy difference between the two rotamers was determined by relative intensity measurements.³⁷ The dipole moment of the gauche rotamer was not determined experimentally owing to insufficient intensities. The ratio of the dipole moments is important, and the theoretical dipole moments shown in Table 1 were used to derive this ratio. Relatively strong isolated lines were used. The statistical weight of gauche was assumed to be twice the weight of the syn conformer. A value of 2.1(4) kJ/mol was derived with syn as the most stable form. The theoretical values for this energy difference is 2.5 (G3; Table 2), 2.1 (MP2/V(Q+d)Z), and 2.1 kJ/mol (B3LYP/6-311G(3df,2pd)). There is thus good agreement between theory and experiment in this case.

Conclusions

There are two stable conformers of allenylphosphine, the more stable syn form and the less stable gauche rotamer. The energy difference is 2.1(4) kJ/mol. This is the same conformational preference as that found in vinylphosphine.⁶ Accurate equilibrium geometries have been derived for the two stable rotamers of allenylphosphine, and for the two corresponding conformers of vinyl phosphine in high-level ab initio calculations. The most important geometrical parameters warrant comments: The C–P bond lengths are slightly longer in allenylphosphine (182.9 pm; Table 5) than in the vinylphosphine conformers (182.4 pm in syn, 181.9 pm in gauche; Table 3). The C=C double bond length in vinylphosphine is 133.5 pm in both forms (Table 3). The two C=C bond lengths are definitely shorter than this in allenylphosphine (130.7 or 130.9 pm; Table 5), which on the other hand is practically the same as in the parent allene molecule.²⁹

Acknowledgment. We thank Anne Horn for her most helpful assistance. A grant from the French-Norwegian Aurora Program to J.-C.G. and H.M. is gratefully acknowledged. J.-C.G. thanks the Centre National d'Etudes Spatiales (CNES) for financial support. H.M. thanks the Research Council of Norway (Programme for Supercomputing) for a grant of computer time.

Supporting Information Available: Assigned MW spectra (Tables 1S–6S); additional results from the quantum chemical

calculations (Tables 7S–10S). This material is available free of charge via the Internet at <http://pubs.acs.org>.

References and Notes

- (1) Groner, P.; Johnson, R. D.; Durig, J. R. *J. Chem. Phys.* **1988**, *88*, 3456.
- (2) Marstokk, K.-M.; Møllendal, H. *Acta Chem. Scand., Ser. A* **1983**, *37*, 755.
- (3) Marstokk, K.-M.; Møllendal, H. *Acta Chem. Scand.* **1996**, *50*, 875.
- (4) Demaison, J.; Guillemin, J.-C.; Møllendal, H. *Inorg. Chem.* **2001**, *40*, 3719.
- (5) Møllendal, H.; Demaison, J.; Guillemin, J.-C. *J. Phys. Chem. A* **2002**, *106*, 11481.
- (6) (a) Dréan, P.; Le Guennec, M.; López, J. C.; Alonso, J. L.; Denis, J. M.; Kreglewski, M.; Demaison, J. *J. Mol. Spectrosc.* **1994**, *166*, 210. (b) Dréan, P.; Colmont, J.-M.; Lesarri, A.; López, J. C. *J. Mol. Spectrosc.* **1996**, *176*, 180.
- (7) Cohen, E. A.; McRae, G. A.; Goldwhite, H.; Di Stefano, S.; Beaudet, R. A. *Inorg. Chem.* **1987**, *26*, 4000.
- (8) Guillemin, J.-C.; Savignac, P.; Denis, J. M. *Inorg. Chem.* **1991**, *30*, 2170.
- (9) Lacombe, S.; Dong, W.; Pfister-Guillouzo, G.; Guillemin, J.-C.; Denis, J. M. *Inorg. Chem.* **1992**, *31*, 4425.
- (10) Ashby, E. C.; Prather, J. *J. Am. Chem. Soc.* **1966**, *88*, 729.
- (11) Guirgis, G. A.; Marstokk, K.-M.; Møllendal, H. *Acta Chem. Scand.* **1991**, *45*, 482.
- (12) Wodarczyk, F. J.; Wilson, E. B., Jr. *J. Mol. Spectrosc.* **1971**, *37*, 445.
- (13) Marstokk, K.-M.; Møllendal, H. *Acta Chem. Scand., Ser. A* **1988**, *42*, 374.
- (14) Waal, Ø., personal communication, 1994.
- (15) Kassı, S.; Petitprez, D.; Włodarczyk, G. *J. Mol. Struct.* **2000**, *517–518*, 375.
- (16) Hampel, C.; Peterson, K. A.; Werner, H. J. *Chem. Phys. Lett.* **1992**, *190*, 1.
- (17) Frisch, M. J.; Trucks, G. W.; Schlegel, H. B.; Scuseria, G. E.; Robb, M. A.; Cheeseman, J. R.; Montgomery, J. A., Jr.; Vreven, T.; Kudin, K. N.; Burant, J. C.; Millam, J. M.; Iyengar, S. S.; Tomasi, J.; Barone, V.; Mennucci, B.; Cossi, M.; Scalmani, G.; Rega, N.; Petersson, G. A.; Nakatsuji, H.; Hada, M.; Ehara, M.; Toyota, K.; Fukuda, R.; Hasegawa, J.; Ishida, M.; Nakajima, T.; Honda, Y.; Kitao, O.; Nakai, H.; Klene, M.; Li, X.; Knox, J. E.; Hratchian, H. P.; Cross, J. B.; Adamo, C.; Jaramillo, J.; Gomperts, R.; Stratmann, R. E.; Yazyev, O.; Austin, A. J.; Cammi, R.; Pomelli, C.; Ochterski, J. W.; Ayala, P. Y.; Morokuma, K.; Voth, G. A.; Salvador, P.; Dannenberg, J. J.; Zakrzewski, V. G.; Dapprich, S.; Daniels, A. D.; Strain, M. C.; Farkas, O.; Malick, D. K.; Rabuck, A. D.; Raghavachari, K.; Foresman, J. B.; Ortiz, J. V.; Cui, Q.; Baboul, A. G.; Clifford, S.; Cioslowski, J.; Stefanov, B. B.; Liu, G.; Liashenko, A.; Piskorz, P.; Komaromi, I.; Martin, R. L.; Fox, D. J.; Keith, T.; Al-Laham, M. A.; Peng, C. Y.; Nanayakkara, A.; Challacombe, M.; Gill, P. M. W.; Johnson, B.; Chen, W.; Wong, M. W.; Gonzalez, C.; Pople, J. A. Gaussian 03, Revision B.03; Gaussian, Inc.: Pittsburgh, PA, 2003.
- (18) Becke, A. D. *J. Chem. Phys.* **1993**, *98*, 5648.
- (19) Lee, C.; Yang, W.; Parr, R. G. *Phys. Rev. B* **1988**, *37*, 785.
- (20) Curtiss, L. A.; Raghavachari, K.; Redfern, P. C.; Rassolov, V.; Pople, J. A. *J. Chem. Phys.* **1998**, *109*, 7764.
- (21) Pople, J. A.; Head-Gordon, M.; Raghavachari, K. *J. Chem. Phys.* **1987**, *87*, 5968.
- (22) Curtiss, L. A.; Carpenter, J. E.; Raghavachari, K.; Pople, J. A. *J. Chem. Phys.* **1992**, *96*, 9030.
- (23) Møller, C.; Plesset, M. S. *Phys. Rev.* **1934**, *46*, 618.
- (24) Meléndez, F. J.; Gallego-Luxan, B.; Demaison, J.; Smayars, Y. G. *J. Comput. Chem.* **2000**, *21*, 1167.
- (25) Purvis, G. D., III; Bartlett, R. J. *J. Chem. Phys.* **1982**, *76*, 1910.
- (26) Raghavachari, K.; Trucks, G. W.; Pople, J. A.; Head-Gordon, M. *Chem. Phys. Lett.* **1989**, *157*, 479.
- (27) (a) Dunning, T. H., Jr. *J. Chem. Phys.* **1989**, *90*, 1007. (b) Dunning, T. H., Jr.; Peterson, K. A.; Wilson, A. K. *J. Chem. Phys.* **2001**, *114*, 9244.
- (28) Margulès, L.; Demaison, J.; Boggs, J. E. *J. Mol. Struct. (THEOCHEM)* **2000**, *500*, 245.
- (29) Margulès, L.; Demaison, J.; Boggs, J. E. *Struct. Chem.* **2000**, *11*, 145.
- (30) McRae, G. A.; Gerry, M. C. L.; Cohen, E. A. *J. Mol. Spectrosc.* **1986**, *116*, 58.
- (31) Margulès, L.; Demaison, J.; Rudolph, H. D. *J. Mol. Struct.* **2001**, *599*, 23.
- (32) Lee, T. J.; Taylor, P. R. *Int. J. Quantum Chem., Quantum Chem. Symp.* **1989**, *23*, 199.
- (33) Peterson, K. A.; Dunning, T. H., Jr. *J. Chem. Phys.* **2002**, *117*, 10548.
- (34) Demaison, J.; Boggs, J. E.; Rudolph, H. D. *J. Mol. Struct.* **2004**, *695–696*, 145.
- (35) Watson, J. K. G. *Vibrational Spectra and Structure*; Elsevier: Amsterdam, 1977; Vol. 6.
- (36) Laurie, V. W.; Herschbach, D. R. *J. Chem. Phys.* **1962**, *37*, 1687.
- (37) Esbitt, A. S.; Wilson, E. B. *Rev. Sci. Instrum.* **1963**, *34*, 901.
- (38) Muentzer, J. S. *J. Chem. Phys.* **1968**, *48*, 4544.